Scientific Research Publishing

Circuits and Systems, 2026, 17(4), 63-81
https://www.scirp.org/journal/cs
ISSN Online: 2153-1293
ISSN Print: 2153-1285

Influence of Excitation Resistance and Synchronization Conditions on the Transient Performance of a Synchronous Motor during Asynchronous Starting

Medhy Kayembe Kazadi

Department of Electrical Engineering, Institut Supérieur des Techniques Appliquées, Kolwezi, Democratic Republic of the Congo
Email: kayembemedy@gmail.com

How to cite this paper: Kazadi, M.K. (2026) Influence of Excitation Resistance and Synchronization Conditions on the Transient Performance of a Synchronous Motor during Asynchronous Starting. *Circuits and Systems*, **17**, 63-81.
https://doi.org/10.4236/cs.2026.174004

Received: March 15, 2026
Accepted: April 27, 2026
Published: April 30, 2026

Abstract

Synchronous motors are widely used in industrial and power-system applications because of their high efficiency, controllable power factor, and excellent steady-state performance. However, their starting process remains a major challenge due to the high transient currents and torque oscillations that occur before synchronization. This study presents a numerical investigation of the asynchronous starting of a synchronous motor using the MATLAB/Simulink environment. A detailed simulation model of an 85 kVA, 400 V, 50 Hz synchronous motor was developed to evaluate its transient and steady-state behavior under different excitation resistance configurations. The influence of additional excitation resistances on excitation voltage, excitation current, electromagnetic torque, stator current, rotor speed, and direct- and quadrature-axis currents was analyzed. The results show that the insertion of an appropriate starting resistance significantly reduces transient current peaks and torque oscillations during startup. Furthermore, applying the excitation voltage when the rotor speed approaches synchronous speed improves synchronization stability and reduces electromechanical stresses. Among the investigated configurations, a starting resistance approximately five times greater than the field-winding resistance provides the most effective balance between voltage limitation and dynamic performance. The proposed simulation approach provides a practical tool for the analysis and optimization of synchronous motor starting strategies in industrial applications.

Keywords

Synchronous Motor, Asynchronous Starting, MATLAB/Simulink, Excitation

Resistance, Transient Analysis, Electromagnetic Torque, Electrical Machine Simulation

1. Introduction

Synchronous machines are widely employed in industrial power systems because of their high efficiency, controllable power factor, excellent steady-state performance, and suitability for large constant-speed applications [1] [2]. These characteristics make synchronous motors particularly attractive for applications requiring constant-speed operation and high-power ratings.

However, the starting process of synchronous motors remains a significant technical challenge. Unlike induction motors, synchronous motors require an additional direct-current excitation system and cannot start directly in synchronism with the rotating stator magnetic field. To address this limitation, several starting techniques have been proposed, including pony motors, variable-frequency drives, static frequency converters, and asynchronous starting using damper windings [3] [4].

Despite its practical advantages, asynchronous starting is often associated with high inrush currents, oscillatory torque, and synchronization instability, which remain major challenges during asynchronous starting, particularly in large industrial synchronous motors [5] [6]. Therefore, understanding the influence of excitation-circuit parameters and synchronization conditions is essential for improving starting performance and ensuring reliable operation of synchronous motors in industrial applications.

Advances in numerical simulation tools have made it possible to analyze the dynamic behavior of electrical machines with high accuracy. Dynamic simulation platforms such as MATLAB/Simulink and Simscape Electrical provide reliable environments for investigating transient electromechanical phenomena before physical implementation [7] [8].

This study investigates the asynchronous starting behavior of a synchronous motor using a MATLAB/Simulink model, with particular emphasis on the influence of excitation resistance and excitation switching conditions on transient performance, synchronization quality, and overall system stability. To investigate the influence of excitation timing, two representative synchronization strategies are analyzed: excitation applied near synchronous speed and excitation applied at an intermediate rotor speed.

2. Synchronous Machine Model and Parameters

The study considers an 85 kVA, 400 V, 50 Hz three-phase synchronous motor supplied from a balanced electrical network. A comprehensive electromechanical model was developed in MATLAB/Simulink using the d-q axis (Park's transformation) representation to simulate the asynchronous starting process and the subsequent transition to synchronous operation. The model incorporates the principal electrical and mechanical characteristics of the machine, including the stator and excitation winding resistances, damper winding parameters, d-q axis inductances, and rotor inertia.

These parameters were assumed constant throughout the simulations to ensure a consistent evaluation of the effects of excitation resistance and synchronization conditions on motor performance. The mathematical model is based on the classical d-q axis representation, which is widely used for the dynamic analysis of synchronous machines [9]-[11]. All machine parameters are expressed in the per-unit system following IEEE recommendations [12] [13].

The principal electrical and mechanical parameters used to develop the synchronous motor model are summarized in **Table 1**. These parameters constitute the basis of all simulation scenarios investigated in this study.

Table 1. Main parameters.

Parameter	Value	Unit
Electrical Network		
Voltage	400	V
Frequency	50	Hz
Phase angle	0	°
Synchronous Machine		
Rated voltage	400	V
Rated frequency	50	Hz
Phase angle	0	°
Inertia constant	1	s
Rated power	85	kVA
Number of pole pairs	2	–
Friction coefficient	0.02032	pu
Excitation voltage	1	pu
Resistances		
Armature resistance, r	0.02922	pu
Field winding resistance, r_f	0.0193	pu
d-axis damper winding resistance, r_D	0.2696	pu

Continued

q-axis damper winding resistance, r_Q	0.06201	pu
Additional field winding resistance, R_x	$f(r_f)$	pu
Inductances		
Stator leakage inductance, l	0.06	pu
d-axis magnetizing inductance, l_{md}	2.14	pu
q-axis magnetizing inductance, l_{mq}	0.95	pu
Field winding magnetizing inductance, l_f	0.2173	pu
d-axis damper winding magnetizing inductance, l_D	0.7235	pu
q-axis damper winding magnetizing inductance, l_Q	0.09942	pu
Load		
Mechanical load torque	0.5	pu
Load application instant (At excitation switching)	$\omega_r \geq 0.99$ or $\omega_r \geq 0.5$	pu
Load model	Constant torque	pu

Machine Parameter Source and Per-Unit System

The synchronous machine parameters used in this study were obtained from the standard MATLAB/Simulink (Simscape Electrical) Synchronous Machine block, representing an 85 kVA, 400 V, 50 Hz three-phase machine. The model is based on the d-q axis representation commonly adopted for transient analysis and validated against established electrical machine theory.

All electrical quantities are expressed in the per-unit (pu) system using the following base values:

- Rated apparent power: $S_{base} = 85$ kVA
- Rated line-to-line voltage: $V_{base} = 400$ V
- Rated frequency: $F_{base} = 50$ Hz
- Rated angular speed: $\omega_{base} = 2\pi f = 314.16$ rad/s
- Base current: $I_{base} = 122.7$ A
- Base impedance: $Z_{base} = 1.882\ \Omega$

The per-unit representation facilitates the comparison of different operating conditions and ensures the reproducibility of the simulation results.

The simulation block diagram integrates:

- Electrical supply network,
- Coupling switch,

- Synchronous motor model,
- Excitation control system,
- Mechanical load model,
- Speed monitoring and synchronization logic.

The complete MATLAB/Simulink implementation developed for this study is presented in **Figure 1**. As shown in **Figure 1**, the model integrates the electrical supply network, synchronous motor, excitation control system, mechanical load, and synchronization logic to reproduce the asynchronous starting and synchronization processes.

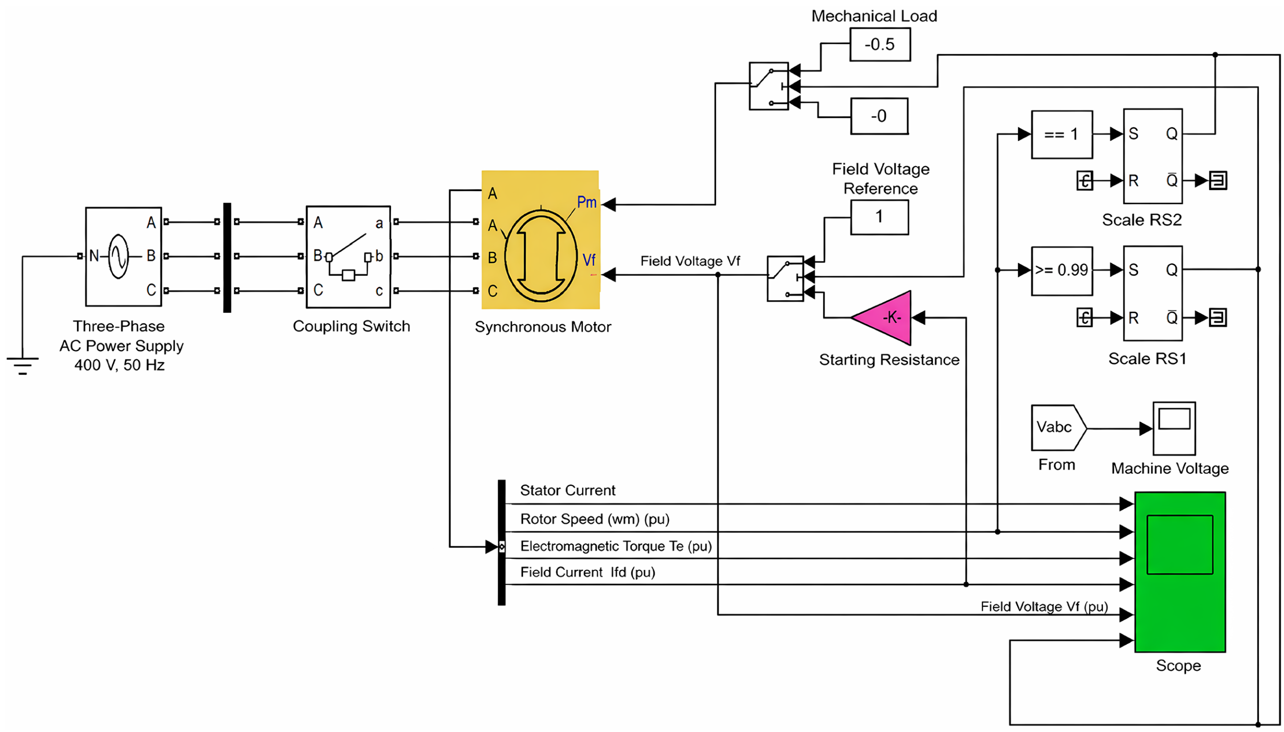

Figure 1. Block diagram of the MATLAB/Simulink model for asynchronous starting of a synchronous motor.

3. Methodology

The simulation methodology follows established dynamic modelling approaches reported in the literature [14]-[16]. The model incorporates the electrical and mechanical characteristics of the machine, including the excitation system, rotor dynamics, and electromagnetic interactions occurring throughout the startup process. All simulations were performed using the same machine parameters and per-unit base quantities defined in Section 2 to ensure consistency and reproducibility of the comparative analysis. The simulation workflow shown in **Figure 1** was used for all investigated operating scenarios, ensuring identical machine parameters and operating conditions throughout the comparative analysis.

The simulation begins at t = 0 s, with the synchronous motor operating in asynchronous mode. During this period, the excitation winding is not energized by the DC excitation source. Instead, an additional resistance (R_x) is connected to the excitation circuit to limit induced voltage and current peaks generated during rotor acceleration. To evaluate the influence of the excitation-circuit resistance on motor performance, three resistance configurations were considered: $R_x = 0$, corresponding to a short-circuited excitation winding, $R_x = 5*r_f$, and $R_x = 10*r_f$, where rf represents the excitation-winding resistance.

The transition from asynchronous operation to synchronous operation is achieved through controlled excitation switching. The DC excitation voltage is applied when the rotor speed reaches a predefined threshold relative to synchronous speed. Two synchronization criteria were investigated: excitation application near synchronous speed ($\omega_r \geq 0.99$ pu) and excitation application at a significantly lower rotor speed ($\omega_r \geq 0.5$ pu). Two synchronization speed thresholds were selected to represent two practical excitation strategies commonly encountered in industrial synchronous motor applications. The threshold $\omega_r \geq 0.99$ pu corresponds to the conventional synchronization practice, where the DC excitation is applied only when the rotor speed is very close to synchronous speed, thereby minimizing slip and reducing electrical and mechanical transients during synchronization. In contrast, the threshold $\omega_r \geq 0.5$ pu represents an earlier excitation strategy intended to evaluate the motor response under higher slip conditions and increased electromechanical interaction. Comparing these two representative operating conditions provides a clear assessment of the influence of excitation timing on transient performance, synchronization quality, and overall system stability. Once the programmed speed threshold is reached, the additional starting resistance is disconnected, the DC excitation voltage is applied to the rotor winding, and the mechanical load is introduced [17]-[19].

In the present study, the synchronization process is based exclusively on a rotor-speed threshold criterion, whereby the DC excitation voltage is automatically applied when the rotor speed reaches the predefined value ($\omega_r \geq 0.99$ pu or $\omega_r \geq 0.5$ pu). Rotor electrical angle and stator phase alignment are not explicitly monitored or controlled prior to excitation switching. This simplified synchronization strategy was intentionally adopted to isolate the effects of excitation resistance and excitation timing on the transient performance of the synchronous motor while avoiding the additional complexity of closed-loop synchronization algorithms. Consequently, successful pull-in to synchronism results from the natural electromechanical interaction between the stator rotating magnetic field and the excited rotor, which is consistent with the operating principle of asynchronous-start synchronous motors.

The mechanical load was represented by a constant load torque model, which is widely adopted for the dynamic analysis of industrial synchronous motor drives. To focus on the influence of excitation resistance and synchronization conditions, the load torque was maintained constant throughout all simulation cases and was applied simultaneously with the DC excitation voltage once the programmed synchronization speed threshold was reached ($\omega_r \geq 0.99$ pu or $\omega_r \geq 0.5$ pu, depending on the investigated case). The load magnitude was set to 0.5 pu, corresponding to approximately 50% of the rated motor torque, thereby representing a typical industrial operating condition while avoiding excessive acceleration disturbances. This configuration ensures that all simulation scenarios are evaluated under identical mechanical conditions and that any observed differences are solely attributable to the excitation resistance and synchronization strategy. The motor subsequently transitions from asynchronous operation to stable synchronous operation [11] [19].

The performance of the proposed starting strategy was evaluated through the analysis of the transient and steady-state responses of the principal electrical and mechanical variables, namely the field excitation voltage, field excitation current, electromagnetic torque, rotor speed, direct-axis current, quadrature-axis current, and armature current. Particular attention was given to the maximum transient values, oscillation characteristics, damping behavior, and synchronization performance under each operating condition.

A comparative analysis of all simulation scenarios was performed to determine the influence of starting resistance and excitation-switching criteria on electrical stress, mechanical performance, and synchronization quality. The results were used to identify the most suitable operating configuration capable of minimizing transient currents, reducing torque oscillations, limiting voltage stress on the excitation winding, and ensuring smooth and reliable synchronization of the synchronous motor.

To verify the reliability of the developed MATLAB/Simulink model, the simulated startup characteristics were qualitatively compared with the classical transient behavior of asynchronous-start synchronous motors reported in established textbooks, published research, and the MATLAB/Simscape Electrical reference model. In all investigated cases, the model reproduced the expected physical phenomena, including high initial stator current, damped electromagnetic torque oscillations, progressive rotor acceleration, and stable pull-in to synchronism following field excitation. The observed reduction in excitation-current peaks and improvement in transient damping with increasing excitation resistance are also consistent with the behavior described by Chapman (2012), Krause *et al.* (2013), IEEE Std 115-2019, and MathWorks (2025). This agreement provides confidence that the developed simulation model accurately represents the transient performance of the investigated synchronous motor.

4. Simulation Results and Discussion

The selected synchronization thresholds ($\omega_r \geq 0.99$ pu and $\omega_r \geq 0.5$ pu) represent conventional and early excitation strategies, respectively, enabling a direct comparison of their effects on transient electrical and mechanical performance.

The obtained transient responses are consistent with the theoretical behavior of asynchronous-start synchronous motors reported in the literature and MATLAB/Simscape Electrical reference models, thereby providing confidence in the physical validity of the proposed simulation model.

- Case 1: Rotor speed $\omega_r \geq 0.99$ p.u. and $R_x = 0\ \Omega$ (without R_x in the circuit).

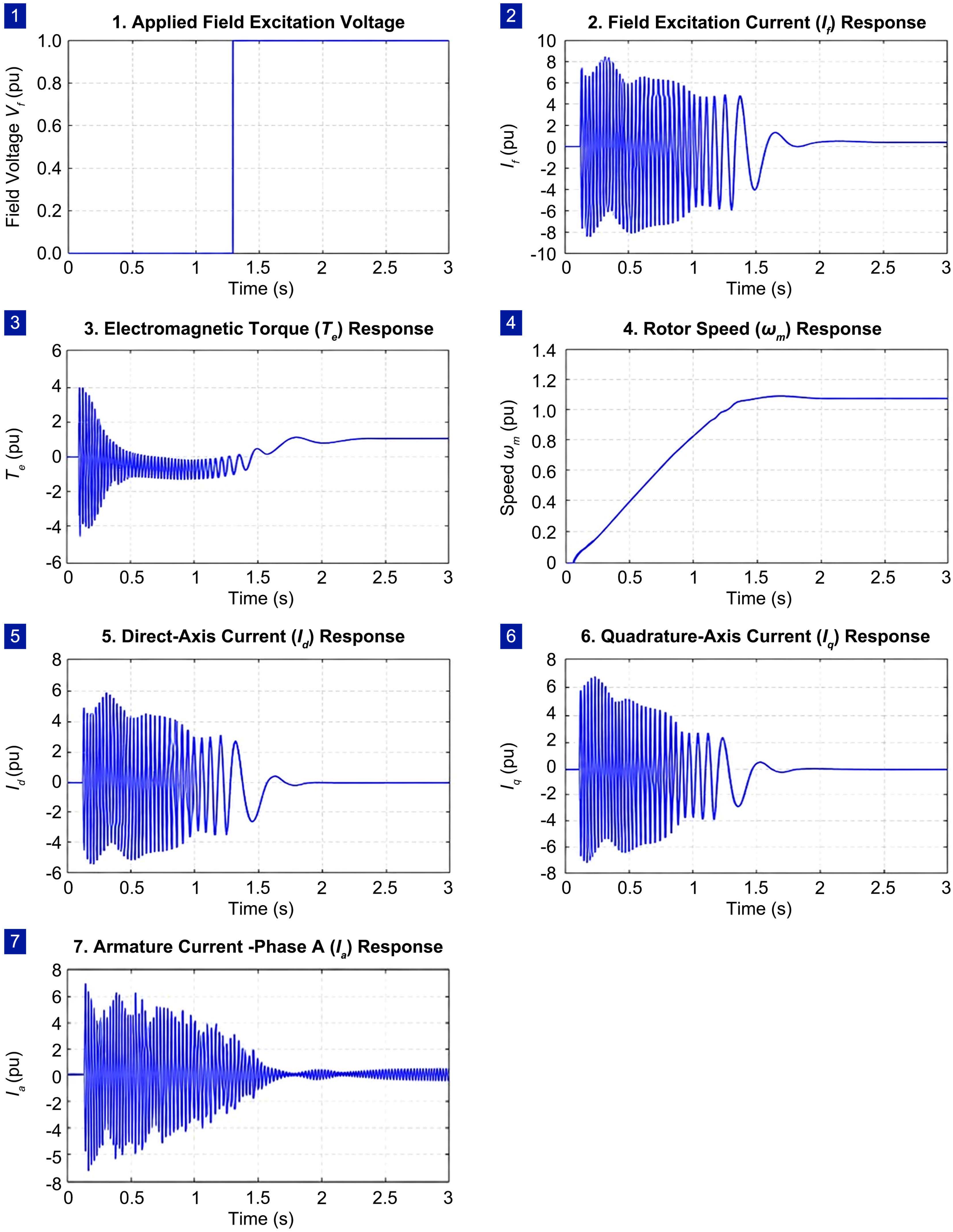

- **Case 2: Rotor speed $\omega_r \geq 0.99$ p.u. and $R_x = 5 \times r_f$.**

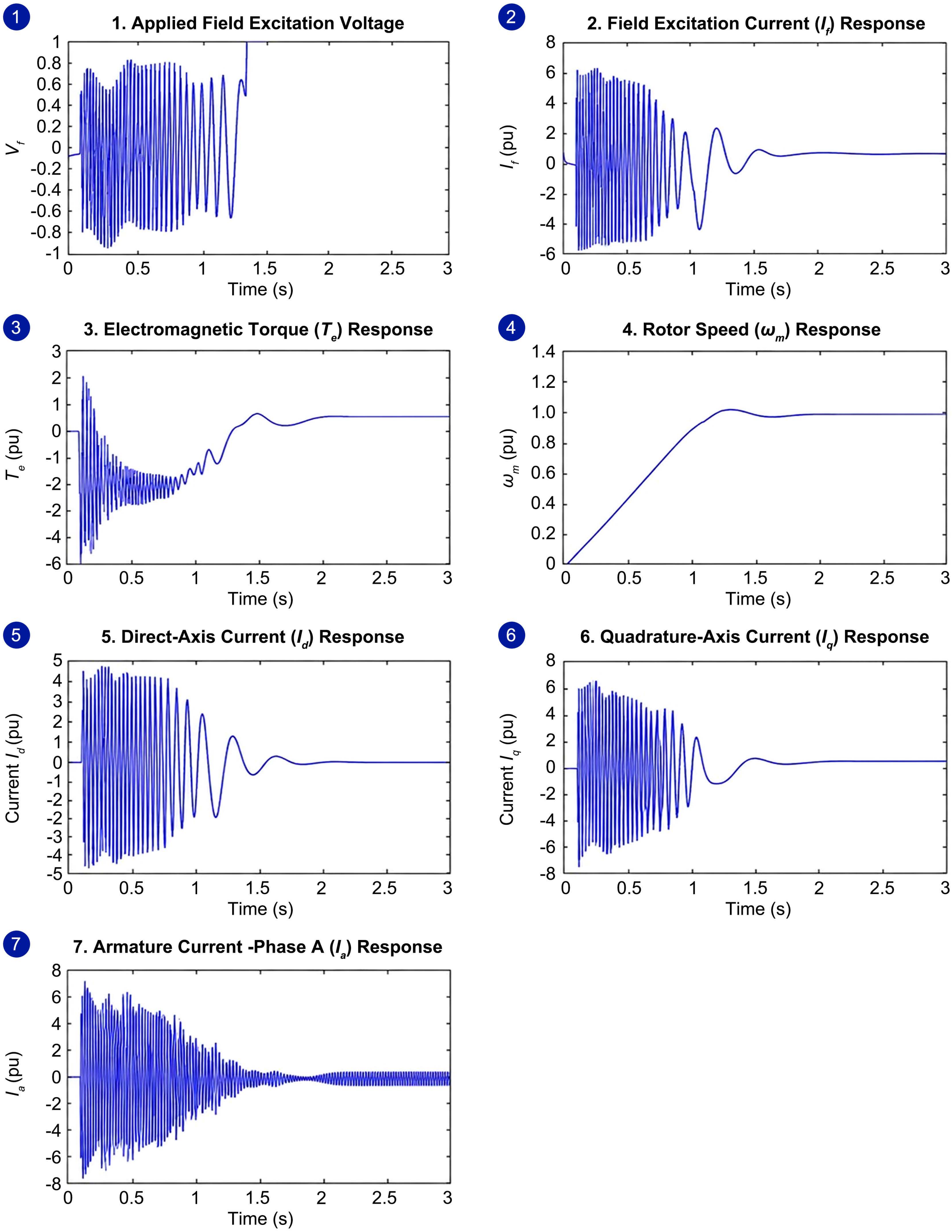

- **Case 3: Rotor speed $\omega_r \geq 0.99$ p.u. and $R_x = 10 \times r_f$.**

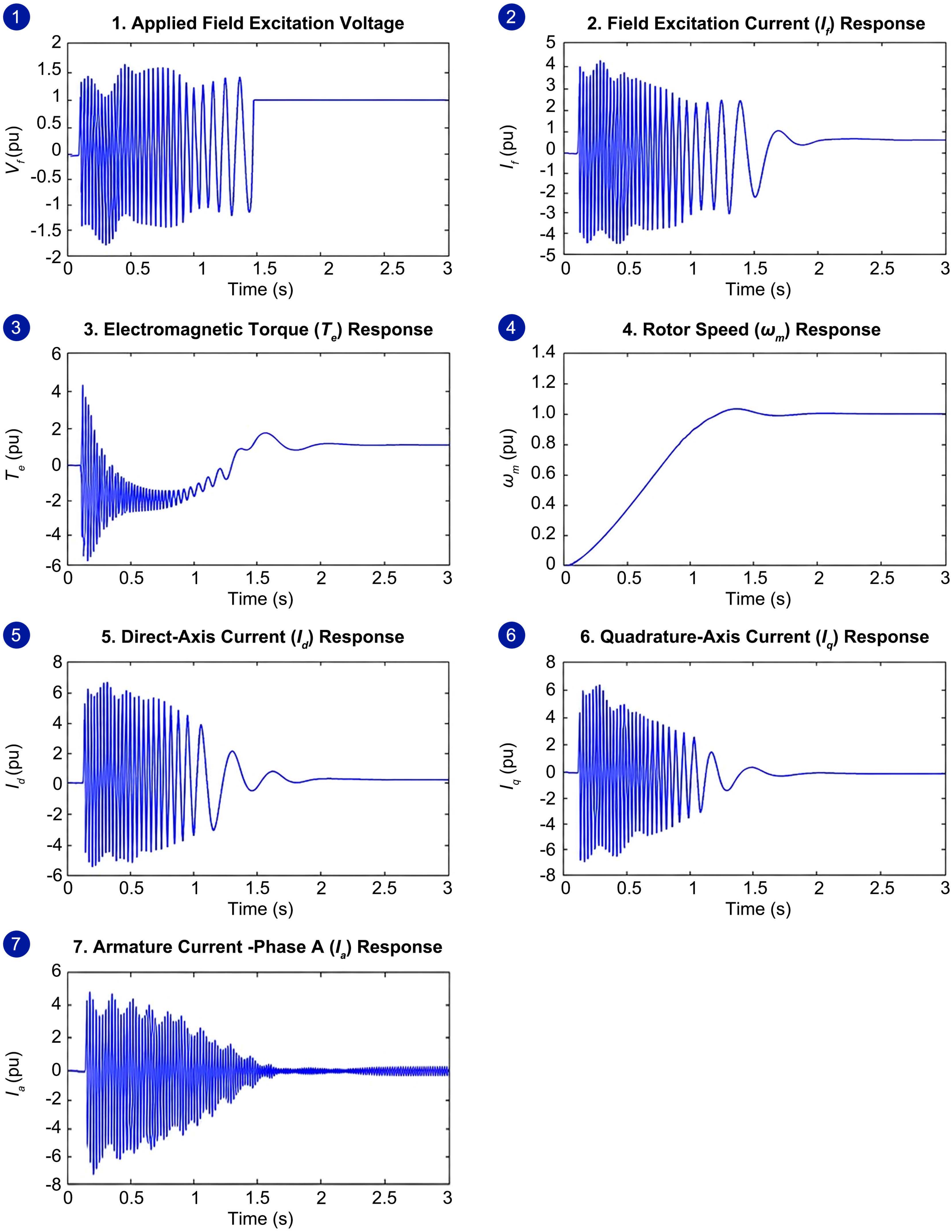

- Case 4: Rotor speed $\omega_r \geq 0.5$ p.u. and $R_x = 5 \times r_f$.

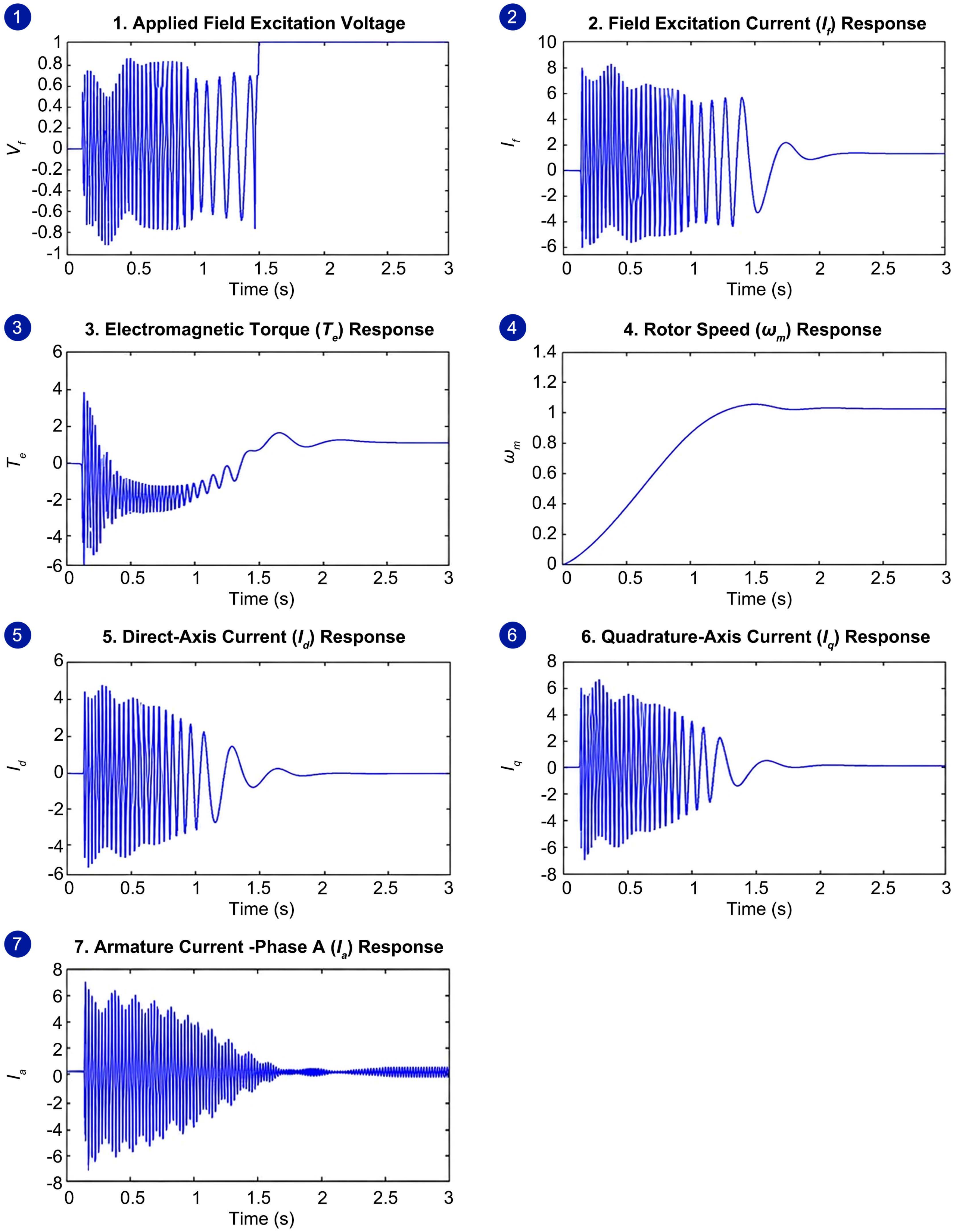

To facilitate comparison among the investigated operating conditions, the principal simulation results obtained for all asynchronous starting scenarios are summarized in Table 2. The table presents the maximum and steady-state values of the main electrical and mechanical variables used throughout the subsequent discussion.

Table 2. Summary of asynchronous starting simulation results for the synchronous motor.

Speed Setpoint	R_x (pu)	vf_{max} (pu)	vf_n (pu)	if_{max} (pu)	If_n (pu)	Ce_{max} (pu)	Ce_n (pu)	id_{max} (pu)	Id_n (pu)	iq_{max} (pu)	iq_n (pu)	ia_{max} (pu)	Ia_n (pu)
$\omega_r \geq 0.99$ pu	0	0	1	9	1	6.7	0.5	6	0	7.2	0.5	7.4	0.5
$\omega_r \geq 0.99$ pu	$5{*}r_f$	0.9	1	6.2	1	5.3	0.5	5	0	7.2	0.5	7.4	0.5
$\omega_r \geq 0.99$ pu	$10{*}r_f$	1.8	1	4.8	1	5.2	0.5	4.3	0	7.2	0.5	7.4	0.5
$\omega_r \geq 0.5$ pu	$5{*}r_f$	0.9	1	9	1	5.3	0.5	5.5	0	7.2	0.5	7.4	0.5

4.1. Influence of Starting Resistance on the Excitation Voltage Response

The transient behavior of the excitation voltage was investigated under different starting resistance values ($R_x = 0$, $5{*}r_f$, and $10{*}r_f$) and excitation switching criteria ($\omega_r \geq 0.99$ pu and $\omega_r \geq 0.5$ pu). During asynchronous startup, the excitation winding remains disconnected from the DC source and is subjected only to the electromotive force induced by rotor motion. As summarized in Table 2, increasing the starting resistance progressively reduces the peak excitation current while increasing the induced excitation voltage, demonstrating the trade-off between current limitation and voltage stress.

The results demonstrate that the starting resistance has a significant influence on the induced voltage developed across the excitation winding. When the excitation winding is short-circuited ($R_x = 0$), the induced voltage remains negligible throughout the asynchronous acceleration period. Once the rotor reaches the prescribed switching speed, the DC excitation source is applied and the field voltage instantaneously reaches its rated value.

The introduction of a starting resistance fundamentally modifies the transient voltage response. The induced voltage exhibits oscillatory behavior whose amplitude increases with the resistance value. While a moderate resistance maintains the induced voltage below the rated insulation level of the excitation winding, excessive resistance results in transient overvoltage that may exceed the nominal excitation voltage. Such overvoltage represents a potential risk to insulation integrity and should therefore be carefully considered during the design stage.

Furthermore, applying excitation at a lower rotor-speed threshold modifies the transient response by initiating synchronization earlier in the acceleration process. However, the simulation results show that this strategy does not significantly reduce the overall time required to reach steady-state operation and is accompanied by a higher excitation-current peak (ifmax = 9 pu for $\omega_r \geq 0.5$ pu compared with 6.2 pu for $\omega_r \geq 0.99$ pu under the same starting resistance $R_x = 5^* r_f$). These findings agree with previous investigations showing that appropriate excitation resistance limits rotor overvoltage while improving synchronization performance [20]-[22]. Therefore, the coordination between excitation timing and starting resistance should primarily aim to minimize transient electrical and mechanical stresses while ensuring reliable synchronization.

4.2. Influence of Starting Resistance on the Excitation Current Response

The excitation current response constitutes one of the most critical indicators of rotor-circuit performance during asynchronous starting. The simulation results reveal that the excitation current is strongly dependent on the starting resistance value. The quantitative results presented in **Table 2** show that the maximum excitation current decreases significantly as the starting resistance increases, confirming the effectiveness of the proposed approach in reducing rotor electrical stress.

Without a starting resistance, the excitation winding is subjected to severe transient currents characterized by high oscillatory amplitudes. These current peaks may accelerate thermal ageing of the winding insulation and increase electromagnetic stresses within the rotor circuit. The application of a starting resistance significantly mitigates these effects by limiting the magnitude of the induced current and improving transient damping.

As the resistance value increases, the peak excitation current decreases substantially, demonstrating the effectiveness of the resistance in controlling rotor-circuit stresses. However, the results also show that excitation timing plays a crucial role. When the DC source is connected before the rotor approaches synchronous speed, a pronounced current surge occurs due to the large slip existing between the rotor magnetic field and the stator rotating field.

From an engineering perspective, the results indicate that proper coordination between the starting resistance and excitation switching criterion is essential to minimize transient current stresses while maintaining acceptable synchronization characteristics. Similar reductions in excitation-current peaks have been reported by Aree and Kerdphol [11] and Zhou *et al.* [11], confirming that optimized excitation resistance improves transient stability.

4.3. Influence of Starting Resistance on Electromagnetic Torque

The electromagnetic torque response provides valuable insight into the electromechanical stability of the synchronization process. During asynchronous startup, significant torque oscillations are generated due to the interaction between stator currents and rotor-induced magnetic fields. According to **Table 2**, the peak electromagnetic torque decreases when a moderate starting resistance is introduced, indicating improved transient stability during synchronization.

The absence of a starting resistance results in the largest torque oscillations and peak torque values. These oscillations may produce undesirable mechanical vibrations, increase fatigue loading on rotating components, and negatively affect the lifespan of couplings, bearings, and driven equipment.

The introduction of a starting resistance significantly improves the transient torque behavior by reducing both the amplitude and frequency of oscillations. This damping effect contributes to smoother acceleration and reduced mechanical stress throughout the starting sequence.

However, the results indicate that increasing the resistance beyond moderate values provides only marginal additional benefits. Consequently, excessively large resistance values may not be justified considering their associated increase in excitation-voltage stress.

When excitation is applied before the rotor approaches synchronous speed, a temporary amplification of torque oscillations is observed. This behavior confirms that synchronization should ideally occur when the slip is sufficiently low to minimize electromechanical disturbances. The reduction in torque oscillations observed in this study is consistent with previous analytical and simulation studies [22]-[24].

4.4. Influence of Starting Resistance on Rotor-Speed Dynamics

The rotor-speed response demonstrates the ability of the synchronous motor to accelerate from standstill and achieve stable synchronous operation. The rotor-speed characteristics summarized in **Table 2** indicate that all investigated configurations successfully reach synchronous speed, although smoother synchronization is achieved when excitation is applied near synchronous speed.

The simulations indicate that the starting resistance has only a minor influence on the overall speed trajectory. Regardless of the resistance value, the machine successfully accelerates and eventually reaches synchronous speed.

The principal effect of the excitation strategy is observed during the synchronization phase. When excitation is applied near synchronous speed, the transition occurs smoothly with minimal disturbance. Conversely, earlier excitation causes a more pronounced acceleration transient before synchronization is achieved.

These results suggest that rotor-speed dynamics are primarily governed by the synchronization mechanism rather than by the magnitude of the starting resistance. Therefore, the resistance selection should be based mainly on electrical and mechanical stress reduction rather than speed-control considerations. These results confirm previous observations that synchronization timing has a greater influence on pull-in behaviour than excitation resistance [24] [25].

4.5. Influence of Starting Resistance on Direct-Axis Current

The direct-axis current represents a key variable associated with rotor magnetic field establishment and synchronization dynamics. During asynchronous startup, substantial oscillations are observed due to the transient interaction between stator and rotor magnetic fields. Table 2 further confirms that increasing the starting resistance reduces the peak direct-axis current, thereby improving transient damping during synchronization.

The results demonstrate that increasing the starting resistance effectively reduces the magnitude of these oscillations and improves current damping. Consequently, the rotor circuit experiences lower electromagnetic stress and improved stability during the transition toward synchronism.

A higher transient peak is observed when excitation is applied before the rotor reaches near-synchronous speed. This phenomenon reflects the increased electromagnetic energy exchange required to force synchronization under higher slip conditions.

The progressive reduction of direct-axis current oscillations following excitation application confirms the successful establishment of a stable rotor magnetic field and the achievement of synchronous operation. This behaviour is consistent with classical d-q axis machine theory [25] [26].

4.6. Influence of Starting Resistance on Quadrature-Axis Current

Unlike the direct-axis component, the quadrature-axis current exhibits limited sensitivity to the starting resistance. The transient waveforms remain remarkably similar for all investigated operating conditions. As shown in Table 2, the quadrature-axis current remains relatively unchanged for all investigated resistance values, indicating limited sensitivity to the excitation resistance.

This behavior suggests that the quadrature-axis current is predominantly controlled by the inherent electromagnetic characteristics of the machine rather than by modifications to the excitation circuit. Although minor differences in damping characteristics can be observed, the overall current magnitude and transient profile remain essentially unchanged.

Following synchronization, the quadrature-axis current stabilizes rapidly, confirming the establishment of steady-state electromechanical equilibrium. Similar trends have been reported in transient machine studies [27] [28].

4.7. Influence of Starting Resistance on Armature Current

The armature current is characterized by a high inrush current immediately following grid connection. This phenomenon is typical of large synchronous machines operating under asynchronous starting conditions. The results summarized in Table 2 indicate that the armature-current peak remains almost constant for all cases, confirming that the stator current is primarily governed by the machine and supply characteristics rather than the excitation-circuit resistance.

The simulation results indicate that the starting resistance has only a limited influence on the maximum armature-current magnitude. Although the oscillatory behavior is slightly attenuated when resistance is introduced into the excitation circuit, the peak stator current remains largely unchanged.

This observation confirms that the armature current is governed primarily by stator impedance, supply voltage, and machine electromagnetic characteristics rather than by the excitation-circuit resistance.

As synchronization is achieved, the armature current progressively converges toward its steady-state value, reflecting the transition from asynchronous to synchronous operation. The armature current behaviour agrees well with IEEE machine performance guidelines [28] [29].

4.8. Engineering Implications and Optimal Starting Configuration

The overall results clearly demonstrate that the starting resistance constitutes an effective means of improving the transient performance of synchronous motors during asynchronous startup. Its implementation significantly reduces excitation-current peaks, attenuates torque oscillations, and improves the damping of direct-axis current transients.

However, excessive resistance values may generate undesirable overvoltages in the excitation winding, thereby increasing insulation stress and potentially compromising long-term reliability.

From a practical engineering perspective, a moderate starting resistance combined with excitation switching near synchronous speed provides the most favorable compromise between electrical stress reduction, mechanical stability, synchronization quality, and equipment reliability. Such a configuration minimizes transient disturbances while ensuring smooth and reliable synchronization, making it the preferred solution for industrial synchronous motor applications.

It should be noted that the present study evaluates synchronization based solely on rotor-speed thresholds. Future work may incorporate rotor electrical angle estimation or phase-alignment algorithms to investigate their influence on pull-in capability, transient oscillations, and synchronization robustness. The recommended starting configuration complies with the transient performance requirements defined in IEC 60034 and IEEE Std 115 [30] [31].

5. General Conclusions

This paper presented a comprehensive dynamic analysis of the influence of excitation resistance and synchronization conditions on the transient performance of a synchronous motor during asynchronous starting using a detailed MATLAB/Simulink model based on the classical d-q axis theory. The developed model successfully reproduced the principal electromechanical phenomena occurring during startup, including excitation voltage and current, electromagnetic torque, rotor speed, direct- and quadrature-axis currents, and armature current. The obtained responses are in good agreement with established synchronous machine theory and international standards for rotating electrical machines [21] [26].

The results demonstrate that synchronization timing and excitation resistance significantly influence the electrical and mechanical performance of the motor. Delaying DC excitation until the rotor reaches near-synchronous speed produces smoother synchronization, lower transient currents, and reduced torque oscillations. Furthermore, the introduction of an external excitation resistance effectively limits field current and improves transient damping. Among the investigated configurations, an excitation resistance of approximately 5*r_f provided the best compromise between current limitation, voltage stress, synchronization stability, and overall dynamic performance, while larger resistance values offered limited additional benefits.

The proposed methodology provides practical guidance for the design and optimization of excitation circuits and synchronization strategies for industrial synchronous motors. By reducing transient electrical and mechanical stresses during startup, the recommended approach can improve system reliability, extend equipment service life, and support more efficient commissioning and operation of medium- and high-power synchronous motor installations.

Overall, this work provides both a scientific contribution to the understanding of synchronous motor transient behavior and a practical engineering framework for optimizing asynchronous starting. Future research should focus on experimental validation, adaptive synchronization techniques, thermal and magnetic saturation effects, and intelligent excitation control to further enhance the reliability and efficiency of industrial synchronous motor drive systems.

Conflicts of Interest

The author declares no conflicts of interest regarding the publication of this paper.

References

[1] Abdessemed, R. (2011) Modélisation et simulation des machines électriques. Ellipses. https://www.editions-ellipses.fr/fr/accueil/464-electrotechnique-modelisation-et-simulation-des-machines-electriques-niveau-c-9782729864958.html

[2] Boldea, I. (2006) Synchronous Generators. CRC Press. https://www.taylorfrancis.com/books/mono/10.1201/b19310/synchronous-generators-ion-boldea

[3] Boldea, I. and Nasar, S.A. (2016) Electric Drives. 3rd Edition, CRC Press. https://doi.org/10.1201/9781315368573

[4] Chapman, S.J. (2012) Electric Machinery Fundamentals. 5th Edition, McGraw-Hill Education. https://books.google.com/books/about/Electric_Machinery_Fundamentals.html?id=wyHAuQAACAAJ

[5] Fitzgerald, A.E., Kingsley, C. and Umans, S.D. (2003) Electric Machinery, 6th Edition, McGraw-Hill.

[6] Krause, P.C., Wasynczuk, O., Sudhoff, S.D. and Pekarek, S. (2013) Analysis of Electric Machinery and Drive Systems. 3rd Edition, John Wiley & Sons. https://doi.org/10.1002/9781118524336

[7] Leonhard, W. (2001) Control of Electrical Drives. 3rd Edition, Springer. https://doi.org/10.1007/978-3-642-56649-3

[8] Ong, C.M. (1998) Dynamic Simulation of Electric Machinery. Prentice Hall. https://engineering.purdue.edu/ECE/Research/Areas/PES/Books/DSEM

[9] Pyrhönen, J., Jokinen, T. and Hrabovcová, V. (2014) Design of Rotating Electrical

Machines. 2nd Edition, Wiley. https://doi.org/10.1002/9781118701591

[10] Sen, P.C. (2014) Principles of Electric Machines and Power Electronics. 3rd Edition, John Wiley & Sons.

[11] Yan, B., Yang, Y. and Wang, X. (2021) A Semi-Numerical Method to Assess Start and Synchronization Performance of a Line-Start Permanent Magnet Synchronous Motor Equipped with Hybrid Rotor. *IET Electric Power Applications*, **15**, 487-500. https://doi.org/10.1049/elp2.12043

[12] Zalas, P. and Zawilak, J. (2011) Gentle Synchronization of Two-Speed Synchronous Motor with Asynchronous Starting. *Electrical Engineering*, **94**, 155-163. https://doi.org/10.1007/s00202-011-0227-1

[13] Carpiuc, S. and Lazar, C. (2017) Modeling of Synchronous Electric Machines for Real-Time Simulation and Automotive Applications. *Journal of the Franklin Institute*, **354**, 6258-6281. https://doi.org/10.1016/j.jfranklin.2017.07.030

[14] Krause, P.C. and Thomas, C.H. (1965) Simulation of Symmetrical Induction Machinery. *IEEE Transactions on Power Apparatus and Systems*, **84**, 1038-1053. https://doi.org/10.1109/TPAS.1965.4766135

[15] Wang, X. and Ren, N. (2003) Simulation of Asynchronous Starting Process of Synchronous Motors Based on MATLAB/Simulink. *Proceedings of the* 6*th International Conference on Electrical Machines and Systems* (*ICEMS* 2003), Vol. 2, Beijing, 1008-1011.

[16] Pillay, P. and Krishnan, R. (1989) Modeling, Simulation, and Analysis of Permanent-Magnet Motor Drives. I. the Permanent-Magnet Synchronous Motor Drive. *IEEE Transactions on Industry Applications*, **25**, 265-273. https://doi.org/10.1109/28.25541

[17] Bose, B.K. (2009) Power Electronics and Motor Drives Recent Progress and Perspective. *IEEE Transactions on Industrial Electronics*, **56**, 581-588. https://doi.org/10.1109/tie.2008.2002726

[18] Kerdphol, T., Rahman, F.S., Watanabe, M. and Mitani, Y. (2019) Robust Virtual Inertia Control of a Low Inertia Microgrid Considering Frequency Measurement Effects. *IEEE Access*, **7**, 57550-57560. https://doi.org/10.1109/access.2019.2913042

[19] Zhao, P., Yao, W., Wen, J., Jiang, L., Wang, S. and Cheng, S. (2015) Improved Synergetic Excitation Control for Transient Stability Enhancement and Voltage Regulation of Power Systems. *International Journal of Electrical Power & Energy Systems*, **68**, 44-51. https://doi.org/10.1016/j.ijepes.2014.12.056

[20] IEC (2022) IEC 60034-1, Rotating Electrical Machines—Part 1: Rating and Performance.

[21] IEC (2018) IEC 60034-4, Rotating Electrical Machines—Part 4: Methods for Determining Synchronous Machine Quantities from Tests.

[22] IEC (2016) IEC 60034-12, Rotating Electrical Machines—Part 12: Starting Performance of Single-Speed Three-Phase Cage Induction Motors.

[23] IEC (2022) IEC 60034-18, Rotating Electrical Machines—Functional Evaluation of Insulation Systems.

[24] IEC (2022) IEC 60034-25, Guidance for the Design and Performance of AC Motors Specifically Designed for Converter Supply.

[25] IEEE (2019) IEEE Std 115-2019, IEEE Guide for Test Procedures for Synchronous Machines.

[26] MathWorks (2026) MATLAB Documentation. https://www.mathworks.com/help

[27] MathWorks (2026) Simulink Documentation.

https://www.mathworks.com/help/simulink

[28] MathWorks (2026) Simscape Electrical Documentation. https://www.mathworks.com/help/physmod/sps

[29] IEEE Xplore Digital Library (2026) Research Database for Electrical Machines and Power Systems. https://ieeexplore.ieee.org

[30] International Electrotechnical Commission (2026) IEC Standards Catalogue. https://www.iec.ch

[31] MathWorks (2026) Simscape Electrical™ User Guide-Synchronous Machine Block Parameters and Per-Unit Representation. https://www.mathworks.com/help/physmod/sps/